Applied Catalysis A: General 392 (2011) 151–157

Contents lists available at ScienceDirect

Applied Catalysis A: General

journal homepage: www.elsevier.com/locate/apcata

# Cobalt–iron magnetic composites as heterogeneous catalysts for the aerobic oxidation of thiols under alkali free conditions

Luciano Menini[1], Márcio C. Pereira, André C. Ferreira, José D. Fabris, Elena V. Gusevskaya*

*Departamento de Química, Universidade Federal de Minas Gerais, Av Antonio Carlos 6627, 31270-901, Belo Horizonte, MG, Brazil*

ARTICLE INFO

*Article history:*
Received 8 September 2010
Received in revised form 1 November 2010
Accepted 2 November 2010
Available online 10 November 2010

*Keywords:*
Cobalt
Magnetic catalysts
Oxidation
Oxygen
Thiols

ABSTRACT

Cobalt–iron magnetic composites prepared by the thermal treatment of an iron oxide-rich soil in the presence of sucrose and cobalt(II) sulfate are efficient heterogeneous catalysts for the liquid-phase aerobic oxidation of thiols into disulfides. The materials have been characterized by Mössbauer spectroscopy, XRD, $N_2$ adsorption–desorption, and elemental analysis. It has been shown that the isomorphic substitution of iron by cobalt occurs preferentially in the framework of the wüstite (FeO) phase and strongly affects the catalytic behavior of the material. The choice of a solvent is critically important for the efficiency of the reaction. In weakly basic solvents, such as dimethylformamide and dimethylacetamide, disulfides can be obtained in near-quantitative yields at low catalyst loading (0.008 mol%). A significant practical advantage of this environment-friendly process is the use of inexpensive magnetically recoverable materials as catalysts and oxygen as a final oxidant as well as mild alkali free conditions. Of particular note are the stability of the catalyst toward leaching and the possibility of catalyst recycling without any special treatment.

## 1. Introduction

Oxidative coupling of thiols (mercaptans) into disulfides is an important reaction in the chemical and petroleum industries [1]. Disulfides are used as key intermediates in a broad range of organic syntheses. They also find various direct industrial applications, e.g. in the vulcanization of rubbers and elastomers. On the other hand, alkyl and aromatic thiols are widely distributed in petroleum products causing foul odor, corrosiveness, and environmental pollution. Thiols should be removed from petroleum before its processing in order to avoid the degradation of metal catalysts; these processes are usually referred to as "sweetening". The oxidation of thiols into innocuous disulfides is the most widely employed procedure in the petroleum refining industry for the removal of thiols (the Merox process) [1].

Due to the weakness and high reactivity of the sulfur–sulfur bond in disulfides, thiols can be easily over-oxidized giving thiosulfinates, thiosulfonates, and sulfonic acids. For this reason, many studies have been focused on the development of adequate conditions for the oxidations of thiols. Most methods reported for the synthesis of disulfides use stoichiometric oxidants, such as dichromates [2,3], permanganates [4], and metal peroxides [5,6]. These processes generate large amounts of undesirable, often toxic, waste by-products and involve complicated work-up procedures. To eliminate such problems, the catalytic oxidation of thiols using molecular oxygen as a final oxidant has been intensively studied in recent years.

The compounds of various elements, such as manganese [7,8], copper [9], vanadium [10], cerium [11], and nickel [12], have been reported to catalyze the aerobic oxidation of thiols into disulfides. However, the most studied catalysts for this reaction are cobalt phthalocyanine complexes. Cobalt phthalocyanines are used in both the petroleum industry for the removal of mercaptans and the commercial-scale syntheses of disulfides [1,13]. Besides the disadvantage of using relatively high price catalysts, these reactions require strongly alkaline conditions to be efficient. For example, in the Merox process, the mercaptans present in petroleum are oxidized with air to disulfides in the presence of water-soluble cobalt phthalocyanines and caustic soda.

Many studies have been directed to the improvement of the homogeneous cobalt phthalocyanine systems [14–16] as well as to the immobilization of cobalt phthalocyanines on solid supports [13,17–21]. In particular, various solid basic materials, such as magnesium containing oxides [17–20] and surface-modified carbons [13], have been tested as supports for these catalysts. Although solid basic catalysts are usually easy to deactivate, it is a valuable approach to avoid the addition of strong soluble bases into the systems and to overcome environmental problems [17].

---

* Corresponding author. Tel.: +55 31 34095741; fax: +55 31 34095700.
*E-mail address:* elena@ufmg.br (E.V. Gusevskaya).

[1] Present address: Coordenadoria do Curso Técnico em Química, Campus Vitória, Instituto Federal do Espírito Santo, 29040-780, Vitória, ES, Brazil.

0926-860X/$ – see front matter © 2010 Elsevier B.V. All rights reserved.
doi:10.1016/j.apcata.2010.11.004

A conventional heterogenization of homogeneous redox systems for using in liquid-phase oxidations usually involves impregnation methods. A main drawback of impregnated catalysts is known to be a solubility of active components in reaction mixtures, i.e. metal leaching. One of the most promising approaches to develop truly heterogeneous catalysts for liquid-phase reactions is the immobilization of redox-active metals in the crystalline structures of inorganic matrices by isomorphic substitution [22]. Besides higher stability towards leaching, these techniques can result in site-isolation of active metal ions in solid matrices, which prevents their aggregation to less reactive species. Such advanced immobilized solid catalysts can show even better catalytic performance than their homogeneous counterparts.

Another important challenge for green chemistry is the development of new technologies for catalyst separation and recycling to substitute traditional time- and solvent-consuming procedures. In this context, the use of magnetic materials as supports in heterogeneous catalysis represents a great advantage providing a convenient route for the catalyst recovery by the application of an external permanent magnet [23–26]. Recently, we have developed magnetic materials through the incorporation of cobalt and manganese ions into framework positions of synthetic ferrites [23,25]. These catalysts were successfully used in the liquid-phase aerobic oxidation of olefins and were stable to leaching.

The aim of the present work was to use an inexpensive iron oxide-rich soil for the preparation of cobalt containing magnetic materials and to study the behavior of these materials as heterogeneous catalysts in liquid-phase oxidation reactions. As a typical starting material, we have chosen a well-characterized red soil sample available in our laboratory. However, in principle, any hematite-rich natural source, such as widespread dark-red geomaterials (soil, rock, or the material from iron ore mines), can be used as a precursor to produce these magnetic catalysts.

We report herein a simple and efficient process for the aerobic oxidation of thiols into disulfides under mild conditions in the absence of alkaline co-catalysts. In this process, cobalt–iron composites easily prepared from low cost cobalt and iron precursors are used as heterogeneous magnetically recoverable catalysts.

## 2. Experimental

All reagents were purchased from commercial sources and used as received, unless otherwise indicated.

### 2.1. Catalyst preparation

The iron oxide-rich soil (itabirite) (ca. 1 g) was impregnated with water (10 mL) containing sucrose (2.5 g) alone or together with $CoSO_4 \cdot 7H_2O$ (0.05, 0.10, or 0.20 g). Then, an aqueous solution of $H_2SO_4$ (0.5 mL, 1:1, vol/vol) was added to accelerate the formation of charcoal and the mixture was heated at 110 °C to evaporate the solvent. The obtained solid was ground and thermally treated for 30 min at 800 °C in air. The resulting samples were denoted as Co0%, Co0.5%, Co1%, and Co2%, in accordance with the determined cobalt content (see below).

### 2.2. Catalyst characterization

The cobalt content was determined by fusing the sample with a $Na_2CO_3$–$K_2CO_3$ mixture, dissolving the fused beads in distilled water, and analysing the solutions on a Spectro Modula ICP-OES instrument.

The chemical analysis of total iron and $Fe^{2+}$ contents was carried out by a photochemical method described by Stucki [27]. The method determines the $Fe^{2+}$ concentration by measuring the $Fe(phen)_3{}^{2+}$ (phen = 1,10-phenantroline) complex after the HF-$H_2SO_4$ digestion of the material. To measure the $Fe^{2+}$ concentration accurately in the presence of $Fe^{3+}$, a sample digestion and analysis were performed under red light to prevent the photochemical reduction of ferric-phenantroline species. A total iron content was measured by photochemical reduction using a fluorescent lamp after the conversion of all $Fe^{3+}$ ions in the digestate to $Fe(phen)_3{}^{2+}$. This procedure avoids the problems associated with the addition of chemical reducing agents to the Fe-phen solutions. Calibration curves were linear up to 8 μg Fe/mL with a lower detection limit of 0.011 μg/mL. The $Fe^{3+}$ content in the composites was calculated as the difference between the total iron content and the $Fe^{2+}$ content.

Surface areas were determined from $N_2$ adsorption isotherms by the BET method using a Autosorb 1 Quantachrome gas sorption analyzer.

X-ray diffraction (XRD) was carried out using Co-Kα radiation with a Rigaku Geigerflex diffractometer equipped with a graphite diffracted-beam monochromator. Data were collected from 10° to 90° $2\theta$ in $2\theta$ steps of 0.02° per 5-s step.

Mössbauer spectra were collected in a constant acceleration transmission mode with a 25 mCi $^{57}Co/Rh$ gamma-ray source. The spectra of the materials were registered at 25 °C. The Doppler velocities ranged between $\pm 10\ mm\ s^{-1}$. The data were stored in a 512-channel MCS memory unit and fitted using the Lorentzian line shapes with a least-squares fitting procedure using the NORMOS program. Isomer shifts were calculated relatively to α-Fe.

### 2.3. Catalytic oxidation experiments

Reactions were carried out in a glass reactor open to air, which was equipped with a condenser and magnetic stirrer. In a typical run, a mixture of the solvent (5 mL), thiol (1–5 mmol), dodecane (0.5 mmol, internal standard), and the catalyst (5 mg, ca. 0.1 wt%) was intensively stirred at 25–50 °C for the indicated time. Reactions were followed by gas chromatography (GC) using dodecane as an internal standard (Shimadzu 17 instrument, Carbowax 20 M capillary column). To take the aliquots for the GC analysis at appropriate time intervals, stirring was stopped and the catalyst was quickly settled by the application of an external permanent magnet. The structures of the products were confirmed by GC/MS (Shimadzu QP2010-PLUS instrument, 70 eV).

Catalyst recycling experiments were performed as follows: after the reaction, the catalyst was magnetically fixed at the bottom of the reactor, then the solution was taken off with a pipette, and the reactor was recharged with the fresh substrate. To control metal leaching, the catalyst was removed at the reaction temperature after the reaction was completed; the solution was recharged with the fresh substrate and allowed to react further.

## 3. Results and discussion

### 3.1. Characterization of the catalysts

The soil used for the preparation of the catalysts is a non-magnetic material with a low surface area ($14\ m^2\ g^{-1}$) extremely rich in iron (57 wt%), that exists exclusively as $Fe^{3+}$ ions. The powder XRD and room-temperature Mössbauer spectroscopy methods indicated that soil mineralogy is dominated by the hematite phase ($\alpha$-$Fe_2O_3$). This phase accounts for 72% of the mass balance, from which 29% is the aluminium substituted hematite. Goethite (α-FeOOH) has been found as an ancillary component (11 wt%) along with several siliceous- and/or aluminium-containing phases: kaolinite (12 wt%), quartz (4 wt%), and gibbsite (1 wt%).

In an attempt to transform the soil in the magnetic material suitable for the preparation of magnetically separable catalysts,

**Table 1**
Data on the amount of iron and iron-containing phases in the catalysts.

| Sample | Iron content (wt%) | | | Phase content (wt%) | | |
|---|---|---|---|---|---|---|
| | $Fe_{total}$ | $Fe^{3+}$ | $Fe^{2+}$ | Hematite | Magnetite | Wüstite |
| Co0% | 29 | 23 | 6 | 10 | 29 | 0 |
| Co0.5% | 30 | 22 | 8 | 8 | 31 | 0 |
| Co1% | 32 | 21 | 11 | 8 | 28 | 4 |
| Co2% | 32 | 19 | 13 | 7 | 24 | 8 |

we have treated the soil at 800 °C in the presence of sucrose. The intention was to reduce $Fe^{3+}$ ions and generate magnetically active phases, such as magnetite ($Fe_3O_4$) or maghemite ($\gamma$-$Fe_2O_3$). The products of the oxidation of sucrose – carbon monoxide and/or charcoal – are expected to act as reducers during the thermal treatment. To incorporate a catalytically active cobalt into the material, $CoSO_4$ was added into the aqueous solution of sucrose in different amounts. Thus, four samples with different contents of cobalt have been prepared: Co0% (no cobalt), Co0.5% (0.5 wt% of cobalt), Co1% (1.0 wt% of cobalt), and Co2% (2.0 wt% of cobalt).

It was found that these materials can be easily recovered from their suspensions by means of an external magnetic field. Thus, hematite and/or goethite have been converted during the treatment, at least partially, into magnetic phases. All other compounds present in the material, such as charcoal and (alumina) silicates, are physically agglomerated with these magnetic particles. In other words, none of the Co0%, Co0.5%, Co1%, and Co2% samples can be magnetically separated into the magnetic and non-magnetic fractions. The whole material (both as-synthesised and after the use several times in the catalytic reaction) can be fixed at the wall of the flask in the proximity of the external permanent magnet leaving behind a transparent liquid.

The total iron content is near 30 wt% in all samples. However, a $Fe^{3+}/Fe^{2+}$ ratio in the samples is different, with the relative amounts of $Fe^{2+}$ being gradually increased with the increase in the cobalt content (Table 1).

The powder XRD (Fig. 1) and room temperature Mössbauer (Fig. 2) analyses indicated the co-existence of two or three crystallographic iron-containing phases in the samples. All materials were found to contain the hematite and magnetite phases. In contrast to Co0%, Co0.5%, the samples with higher cobalt content, i.e. Co1% and Co2%, also contained a non-magnetic phase of wüstite (FeO). None of the samples revealed the phase of goethite. Thus, the treatment of the original soil resulted in the partial reduction of the $Fe^{3+}$ ions and partial transformation of the hematite phase into the magnetite and/or wüstite phase as well as in the complete disappearance of goethite. Preliminary studies carried out with iron-rich soils from other natural sources indicated that the treatment described above resulted in the magnetic materials with a similar phase composition.

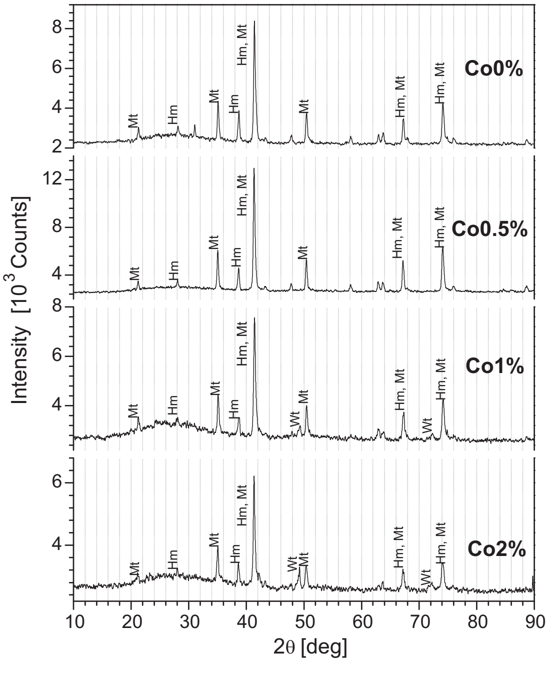

**Fig. 1.** Powder X-ray diffraction patterns of the catalysts. Hm: hematite; Mt: magnetite and Wt: wüstite.

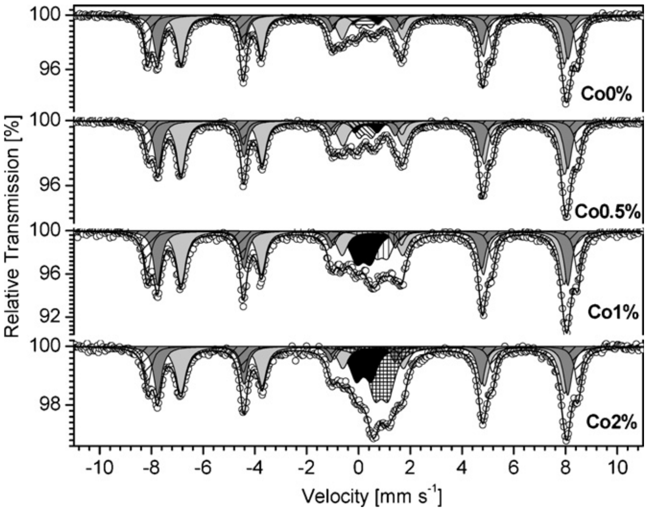

**Fig. 2.** Room temperature Mössbauer spectra of the catalysts.

No formation of individual cobalt oxides was detected in all samples. The incorporation of cobalt seems to occur through the isomorphic substitution of iron in the crystalline structure of the material (as discussed below). The amorphous behavior of all samples observed within the 24–34° 2$\theta$ region should be due to the presence of amorphous charcoal.

In a stoichiometric magnetite, $Fe_3O_4$, all $Fe^{2+}$ ions typically occupy octahedral positions, whereas $Fe^{3+}$ ions are distributed equally between tetrahedral and octahedral sites. Thus, a typical formula for a stoichiometric magnetite can be presented as $[Fe^{3+}]\{Fe^{2+}\ Fe^{3+}\}O_4$, where [ ] and { } denote tetrahedral and octahedral coordination sites, respectively. Fast electron hopping at room temperature, which is known to be a pair-localized phenomenon in octahedral sites of magnetite, results in $Fe^{2.5+}$ from equal amounts of octahedral $Fe^{2+}$ and $Fe^{3+}$, yielding the following formula for the material: $[Fe^{3+}]\{Fe_2{}^{2.5+}\}O_4$.

The room temperature Mössbauer spectra for all samples (Fig. 2) showed the presence of one sextet corresponding to hematite, two sextets assignable to $Fe^{3+}$ in tetrahedral and $Fe^{2.5+}$ in octahedral sites of magnetite, and $Fe^{3+}$ doublets that can be assigned to hematite with small particle size (Table 2). In addition to these phases, wüstite (FeO) was observed in the Co1% and Co2% samples as an internal $Fe^{2+}$ doublet.

It is well reported in the literature that cobalt preferentially replaces iron in the octahedral sites of the magnetite spinel structure [23,25]. However, for the cobalt-containing materials obtained in the present work, the isomer shift ($\delta$) for iron in the octahedral sites of magnetite was practically the same as that for the non-doped sample (Table 2). Moreover, no significant changes in the magnetic hyperfine field and in the ratio between the octahedral and tetrahedral sites occupancies ($R_{oct/tetr}$) were verified. The $R_{oct/tetr}$ values varied between 1.3 and 1.4 in all samples regardless

**Table 2**
Mössbauer parameters obtained from the fit of the room temperature spectra[a].

| Sample | $^{57}$Fe site | $\delta$ (mm s$^{-1}$) | $2\varepsilon$, $\Delta$ (mm s$^{-1}$) | $B_{hf}$ (T) | $\Gamma$ (mm s$^{-1}$) | RA (%) |
|---|---|---|---|---|---|---|
| Co0% | Fe$^{3+}$ | 0.38 | 0.96 | | 0.45 | 4 |
| | Fe$^{3+}$ | 0.35 | 0.50 | | 0.45 | 4 |
| | {Magnetite} | 0.66 | 0.02 | 46.0 | 0.50 | 40 |
| | [Magnetite] | 0.28 | 0 | 49.2 | 0.40 | 29 |
| | Hematite | 0.37 | −0.19 | 51.6 | 0.26 | 23 |
| Co0.5% | Fe$^{3+}$ | 0.40 | 0.86 | | 0.45 | 4 |
| | Fe$^{3+}$ | 0.38 | 0.50 | | 0.45 | 6 |
| | {Magnetite} | 0.67 | −0.02 | 45.9 | 0.53 | 43 |
| | [Magnetite] | 0.28 | 0 | 49.1 | 0.36 | 29 |
| | Hematite | 0.39 | −0.19 | 51.5 | 0.32 | 18 |
| Co1% | Fe$^{3+}$ | 0.31 | 0.54 | | 0.65 | 12 |
| | Wüstite | 1.02 | 0.43 | | 0.55 | 8 |
| | {Magnetite} | 0.66 | 0.01 | 45.9 | 0.55 | 36 |
| | [Magnetite] | 0.28 | −0.01 | 49.2 | 0.34 | 26 |
| | Hematite | 0.37 | −0.19 | 51.6 | 0.32 | 18 |
| Co2% | Fe$^{3+}$ | 0.31 | 0.58 | | 0.60 | 11 |
| | Wüstite | 1.00 | 0.51 | | 0.65 | 17 |
| | Fe$^{2.5+}$ | 0.74 | 0.95 | | 0.45 | 2 |
| | {Magnetite} | 0.67 | −0.02 | 46.0 | 0.50 | 31 |
| | [Magnetite] | 0.28 | 0 | 49.1 | 0.34 | 23 |
| | Hematite | 0.38 | −0.20 | 51.6 | 0.34 | 16 |

[a] $\delta$ – isomer shift with respect to αFe; $\varepsilon$ – quadrupole shift; $\Delta$ – quadrupole splitting; $B_{hf}$ – magnetic hyperfine field; $\Gamma$ – full width at half maximum; RA – relative sub-spectral area; [ ] and { } – representations for tetrahedral and octahedral coordination sites in the spinel structure of magnetite, respectively.

of the cobalt content. This parameter was calculated taking into account that recoilless fractions for octahedral sites were 6% lower than those for tetrahedral sites [28]. These results indicated that iron in the magnetite phase of our material was not replaced by cobalt to an appreciable extent.

The powder XRD results are consistent with the Mössbauer data. No significant changes in the cubic lattice parameter of magnetite (obtained by the Rietveld structural refinement) occurred in the presence of cobalt. The values were 8.3945, 8.3938, and 8.3920 Å for Co0.5%, Co1%, and Co2%, respectively, vs. 8.3920 Å for Co0%.

The Mössbauer parameters of the hematite phase in all samples have not also been influenced by the presence of cobalt (Table 2). On the other hand, significant changes were observed in the wüstite phase (Table 2). The values of quadrupole splitting for wüstite in Co1% and Co2% (0.43 and 0.51 mm s$^{-1}$, respectively) were strongly higher than that expected for non-substituted wüstite (0.21 mm s$^{-1}$ [29]). This could be explained by the structural distortions caused by the isomorphic substitution of Fe$^{2+}$ by Co$^{2+}$ in the framework positions of wüstite. Thus, we believe that in our materials cobalt has replaced the Fe$^{2+}$ ions mainly in the wüstite phase, at least in the Co1% and Co2% samples.

Although wüstite itself is a non-magnetic compound, it seems to be firmly attached to magnetite-containing particles as it can be removed by an external magnet together with the whole material. We believe that our composites contain the particles of hematite coated by magnetite and wüstite, which are formed due to the surface reduction of Fe$^{3+}$ during the thermal treatment of the original soil.

BET surface area measurements have revealed that all samples present the adsorption isotherms characteristic of macroporous materials and show a similar surface area of ca. 40 m$^2$ g$^{-1}$. The distribution of iron-containing phases was estimated using the chemical analysis and Mössbauer spectroscopy data (Table 1). The non-doped Co0% material contains 29 wt% of magnetite and 10 wt% of hematite; whereas the Co2% sample contains 24 wt% of magnetite, 7 wt% of hematite, and 8 wt% of wüstite. The wüstite phase was found to be unstable below 570 °C due to the decomposition into the metallic iron and magnetite [30,31]. However, it has been shown that the presence of calcium can stabilize the wüstite structure and prevent its decomposition [32]. Cobalt seems to exert a similar stabilizing effect in our materials as the higher the cobalt content in the sample the larger amounts of the wüstite phase it contains (Table 1).

### 3.2. Catalytic studies

The oxidation of thiophenol (**1a**), 4-methylthiophenol (**2a**), 4-methoxythiophenol (**3a**), and 4-fluorthiophenol (**4a**) was performed in various solvents in the presence of the Co0%, Co0.5%, Co1%, and Co2% composites. In all experiments, these materials alone were utilized as catalysts under one atmosphere of air without the addition of alkaline co-catalysts, which are usually used in the cobalt catalyzed oxidation of thiols. Results are presented in Tables 3–5.

In blank reactions in dimethylformamide (DMF) with no catalyst added, thiophenol underwent a slow oxidation with air (Table 3, runs 1 and 2). In the presence of the non-doped Co0% material, the conversions of thiophenol were virtually as low as in blank reactions (Table 3, runs 3 and 4). On the other hand, the cobalt-containing samples effectively catalyzed the oxidation of thiophenol and some other thiols (see below) in DMF. The selectivities for corresponding disulfides were virtually 100% with no even trace amounts of other products being detected by GC (Scheme 1). The GC mass balance was based on the substrate charged using dodecane as an internal standard.

The materials can be re-used several times without a significant loss of activity and selectivity. It is important that there is no need to remove the catalyst from the reactor: it can be fixed on the glass walls using an external hand magnet. Then, the solution can be taken off with a pipette and the reactor can be recharged with the fresh substrate dissolved in a suitable solvent. Such a simple handling represents an attractive feature of the developed process.

The oxidation of thiophenol (**1a**) in DMF in the presence of Co.0.5% occurred smoothly at 50 °C resulting in a complete conversion for 4 h to give exclusively diphenyl disulfide (**1b**) (Table 3, run 5). The result of this run corresponded to a turnover number (TON) of 2360 with respect to the total amount of cobalt in the material. However, a real efficiency of the surface cobalt species was much higher as most of the cobalt ions were obviously located in the bulk solid and were not accessible to the substrate. The kinetic

**Table 3**
Cobalt-catalyzed oxidation of thiophenol (**1a**) into diphenyl disulfide (**1b**) in DMF[a].

| Run | Catalyst | Temperature (°C) | Time (h) | Conversion (%) | TON[b] | TOF[b] (min$^{-1}$) | Disulfide yield (%) |
|---|---|---|---|---|---|---|---|
| 1 | None | 25 | 5 | <5 | | | <5 |
| 2 | None | 50 | 4 | 18 | | | 18 |
| 3 | Co0% | 25 | 5 | <5 | | | <5 |
| 4 | Co0% | 50 | 4 | 15 | | | 15 |
| 5 | Co0.5% | 50 | 4 | 100 | 2360 | 9.8 | 100 |
| 6 | Co1% | 50 | 3 | 98 | 1156 | 6.4 | 98 |
| 7 | Co2% | 50 | 1 | 100 | 590 | 9.8 | 100 |
| 8 | Co2% | 25 | 3 | 100 | 590 | 3.3 | 100 |
| 9[c] | Co2% | 50 | 1 | 100 | 3540 | 49.2 | 100 |
| | | | 1 | 100 | 6490 | 49.2 | 100 |
| | | | 1.5 | 100 | 9440 | 33.3 | 100 |
| | | | 2 | 100 | 12,390 | 24.6 | 100 |
| 10[d] | Co2% | 50 | 1 | 100 | 590 | 9.8 | 100 |
| 11[e] | Co2% | 25 | 3 | <3% | | | <3% |

[a] Conditions: $C_6H_5SH$ (0.2 M, 1 mmol), catalyst (0.1 wt%), 1 atm (air). Conversion, selectivity, and yield were determined by GC. In all runs, selectivity for diphenyl disulfide was nearly 100%.

[b] TON – moles of the substrate converted/moles of Co. TOF – the average turnover frequency. TON and TOF were calculated with respect to the total amount of cobalt.

[c] After run 7, four fresh portions of the substrate (5 mmol each) were added consequently, each one after the complete conversion of the previous portion. Total TON is given.

[d] The catalyst was re-used after run 9; TON is given for the second reaction cycle.

[e] After run 8, the catalyst was removed, the solution was recharged with the fresh substrate (1 mmol) and the reaction was allowed to proceed further.

**Table 4**
Cobalt-catalyzed oxidation of thiols in DMF[a].

| Run | Substrate | Temperature (°C) | Time (h) | Disulfide | Yield (%) |
|---|---|---|---|---|---|
| 1 | $C_6H_5SH$ (**1a**) | 25 | 3 | **1b** | 100 |
| 2 | $C_6H_5SH$ (**1a**) | 50 | 1 | **1b** | 100 |
| 3 | 4-$MeC_6H_5SH$ (**2a**) | 25 | 1 | **2b** | 100 |
| 4 | 4-$MeC_6H_5SH$ (**2a**) | 50 | 0.5 | **2b** | 100 |
| 5 | 4-$MeOC_6H_5SH$ (**3a**) | 25 | 1 | **3b** | 100 |
| 6 | 4-$MeOC_6H_5SH$ (**3a**) | 50 | 0.5 | **3b** | 100 |
| 7 | 4-$FC_6H_5SH$ (**4a**) | 50 | 2.5 | **4b** | 100 |

[a] Conditions: substrate (0.2 M, 1 mmol), catalyst Co2% (0.1 wt%), solvent DMF, 1 atm (air). Yield was determined by GC.

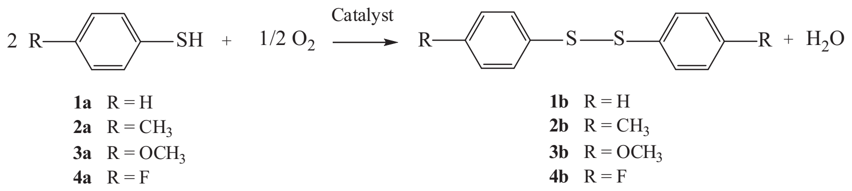

**Scheme 1.** Oxidation of thiols **1a**–**4a** into disulfides **1b**–**4b**.

curves for the oxidation of thiophenol over different catalysts are presented in Fig. 3. The increase in the cobalt content resulted in a near-proportional increase in the reaction rate (Table 3, runs 5–7, Fig. 3). With Co2%, the reaction was completed in 1 h with the average turnover frequency (TOF) of nearly 10 min$^{-1}$ and resulted in the quantitative yield of disulfide. The catalyst was active even at room temperature as the complete conversion of the substrate occurred in 3 h (Table 3, run 8).

In some experiments, the reactor was connected through a capillary tube to a gas burette filled with pure oxygen to avoid a rapid diffusion. An oxygen uptake was observed in these runs in the amounts corresponding to stoichiometry shown in Scheme 1. On the other hand, no reaction occurred under argon, as expected.

It is important to note that the kinetic curves for the reaction are nearly straight lines from 0% to almost 100% conversion. This indicates that the substrate competes successfully for catalyst sites with all other species present in the reaction mixture. In other words, the substrate reacts with cobalt quite readily and most surface cobalt centers, even at high conversions, are bound to thiol or to the fragments derived from thiol. The linearity of the kinetic curves also indicates that the catalysts maintain their activity during the whole reaction course.

**Table 5**
Cobalt-catalyzed oxidation of thiophenol (**1a**) into diphenyl disulfide (**1b**) in various solvents[a].

| Run | Solvent | $\varepsilon$ | Conjugated acid | p$K_a$ | Time (h) | Conversion (%) |
|---|---|---|---|---|---|---|
| 1 | DMF | 36.7 | DMF·$H^+$ | −0.5 | 1 | 100 |
| 2 | DMA | 37.8 | DMA·$H^+$ | −0.5 | 8 | 97 |
| 3 | $CH_3CN$ | 37.5 | $CH_3CNH^+$ | −10 | 4 | 10 |
| 4 | Iso-octane | 1.9 | – | – | 6 | 0 |
| 5 | $C_2H_5OH$ | 24.5 | $C_2H_5OH_2^+$ | −2 | 4 | 95 |

[a] Conditions: $C_6H_5SH$ (0.2 M, 1 mmol), catalyst Co2% (0.1 wt%), 50 °C, 1 atm (air). Conversion was determined by GC. In all runs, selectivity for diphenyl disulfide was nearly 100%. Dielectric constants ($\varepsilon$) are given for the solvents and approximate p$K_a$ values for the corresponding conjugated acids (relative to water [33]).

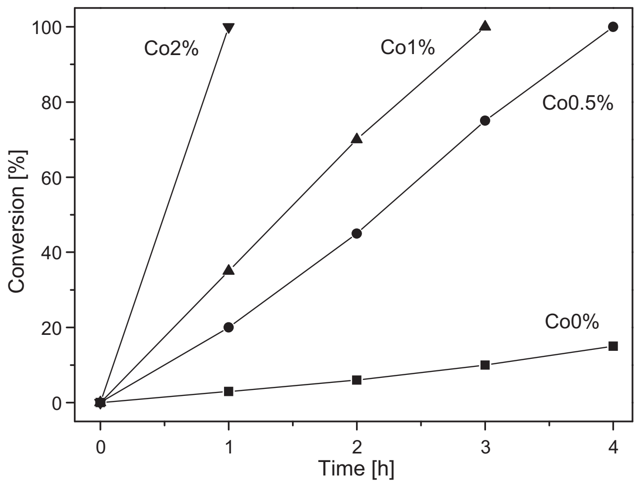

**Fig. 3.** The oxidation of thiophenol in DMF over different catalysts. Conditions: $C_6H_5SH$ (0.2 M, 1 mmol), catalyst (0.1 wt%), 50 °C, 1 atm (air).

To evaluate the catalyst stability and improve its efficiency in terms of TONs, we increased 20 times the amounts of the substrate charged (Table 3, run 9). After the reaction with 1 mmol of the substrate (Table 3, run 7), four 5 mmol substrate portions were added sequentially into the reactor, with each portion being added after the complete conversion of the previous one. The first and the second portions were consumed for 1 h with the average TOF of nearly 50 $min^{-1}$. Thus, each one of these reactions was completed for about the same time as the original reaction with 1 mmol of the substrate (Table 3, run 7). Then, the reaction became slower: for 1 h, in the third reaction it was consumed 80% of the substrate and in the fourth reaction 65%. However, even the fourth portion was consumed for 2 h which corresponds to the average TOF of nearly 25 $min^{-1}$. Overall, the catalyst converted 12,390 mol of the substrate per mol of cobalt, without the separation or any additional treatment.

In run 9 (Table 3), the final product was obtained in the concentration of ca. 30 wt%, which is also one of the technological advantages of the method. On the other hand, such a high content of disulfide in the reaction mixture seems to make the catalyst sites less accessible for the substrate as the reaction slows down. However, the catalyst can be re-used after the removal of the supernatant solution without any further specific treatment or washing. After run 9, the catalyst was magnetically fixed at the bottom of the reactor and the solution was taken off with a pipette. A behavior of the spent catalyst with the fresh substrate was nearly the same as that in the original reaction (Table 3, cf. runs 7 and 10).

To control leaching of the active metal, the catalyst after run 8 was removed; the transparent solution was recharged with the fresh substrate and allowed to react further (Table 3, run 11). Practically no conversion of thiophenol was observed after catalyst removing. This result supports heterogeneous catalysis, i.e. the reaction solution contains no significant amounts of the dissolved cobalt species so that cobalt ions immobilized in the solid matrix are responsible for the substrate oxidation. Thus, the catalyst releases no cobalt to the medium and can be easily recovered either magnetically or by centrifugation and re-used.

The reactivity of various aromatic thiols was examined to evaluate a substrate scope (Table 4). Thiophenols having electron donating groups, such as 4-methylthiophenol (**2a**) and 4-methoxythiophenol (**3a**), underwent oxidation at high rates, even higher than thiophenol itself (Table 4, runs 1 and 2 vs. runs 3–6). On the other hand, the reaction with 4-fluorthiophenol (**4a**), which has an electron withdrawing substituent, occurred slower than that with thiophenol (Table 4, run 2 vs. run 7). All these reactions gave corresponding disulfides **2b**–**4b** in near-quantitative yields and occurred under mild conditions and atmospheric air pressure.

$$\mathrm{RSH} + \mathrm{Solvent} \rightleftharpoons \mathrm{RS^-} + \mathrm{Solvent \cdot H^+}$$
$$2\,\mathrm{Co^{2+}} + 1/2\,\mathrm{O_2} + 2\,\mathrm{Solvent \cdot H^+} \longrightarrow 2\,\mathrm{Co^{3+}} + \mathrm{H_2O} + 2\,\mathrm{Solvent}$$
$$\mathrm{RS^-} + \mathrm{Co^{3+}} \longrightarrow \mathrm{Co^{2+}} + \mathrm{RS\bullet}$$
$$2\,\mathrm{RS\bullet} \longrightarrow \mathrm{RSSR}$$

Overall reaction:

$$2\,\mathrm{RSH} + 1/2\,\mathrm{O_2} \longrightarrow \mathrm{RSSR} + \mathrm{H_2O}$$

**Scheme 2.** Suggested mechanism of the oxidation of thiols over cobalt catalysts.

Further studies revealed a remarkable effect of solvent on the reactivity of thiols in the presence of cobalt–iron composites and brought some light on understanding the reaction mechanism. The results of the oxidation of thiophenol in various solvents are presented in Table 5. The data on polarity (dielectric constants) of the solvents and approximate $pK_a$ values for corresponding conjugated acids are also given in Table 5.

In dimethylacetamide (DMA), the reaction proceeded similarly to that in DMF, albeit slower (Table 5, runs 1 and 2). Both, DMF and DMA, are highly polar solvents with a relatively high basicity ($pK_a \approx -0.5$ for both DMF·$H^+$ and DMA·$H^+$ [33]). In acetonitrile, the solvent with a similar dielectric constant but much less basic ($pK_a \approx -10$ for $CH_3CNH^+$ [33]), the oxidation of thiophenol proceeded very slowly (Table 5, run 3). Thus, the activity of the cobalt–iron composites in the oxidation of thiols depends on solvent basicity rather than its polarity. The reaction did not occur in nonbasic solvents, either polar (acetonitrile) or nonpolar (iso-octane, run 4 in Table 5). On the other hand, in amphiprotic ethanol, which is less polar but much more basic than acetonitrile ($pK_a \approx -2$ for $C_2H_5OH_2{}^+$ [33]), thiophenol reacted rather smoothly, though at a lower rate than in DMF (Table 5, cf. runs 1 and 5). It should be mentioned that no products of the solvent oxidation have been observed in all experiments.

It is generally accepted that the mechanism of the oxidation of thiols into disulfides over cobalt phthalocyanines (the Merox process) consists of three major steps [16,18,20]. First, thiol (RSH) is converted into a thiolate anion ($RS^-$) via the interaction with a basic catalyst ($OH^-$). Then, the one-electron oxidation of $RS^-$ by $Co^{3+}$ gives thiyl radicals ($RS^\bullet$), whose further dimerization results in disulfides. As the $RS^-$ anion coordinates with cobalt more strongly than RSH, the first step should be of a critical importance for the whole process.

Within this approach, it becomes clear why the solvent nature affects so profoundly the reactivity of thiol in our system. A suggested mechanism for the oxidation of thiols over the cobalt–iron composites is presented in Scheme 2. Basic solvents, such as DMF and DMA, favor the deprotonation of the substrate owing to their relatively strong proton-acceptor properties. The protons are then captured at the oxidation of $Co^{2+}$ into $Co^{3+}$ by molecular oxygen to form water. The reduction of the thiolate anion by $Co^{3+}$ regenerates the catalyst and gives $RS^\bullet$ radicals. Finally, the recombination of the $RS^\bullet$ radicals results in disulfide. The weak basicity of acetonitrile and iso-octane strongly prejudices the substrate activation by deprotonation, which seems to be a key step of the whole process. The reaction virtually does not occur in those solvents.

DMA is expected to be more basic than DMF due to the electron donating effect of the additional methyl group. Therefore, the fact that the reaction is much faster in DMF than in DMA is surprising. A possible explanation might be a less steric difficulty for RSH to interact with DMF than with DMA, which would result in more facile deprotonation of RSH in DMF. Anyway, the use of

DMF and DMA as solvents for the oxidation of thiols is an excellent practical proposition for applications due to the advantage of high boiling points of these solvents (152 and 166 °C, respectively) and possibility to obtain high product yields at very low catalyst loadings.

Considering the importance of the substrate activation step, it also becomes clear why the substrates with electron donating groups react faster than thiophenol itself. On the other hand, the presence of electron withdrawing substituents in the aromatic ring slows down the reaction.

## 4. Conclusions

We have developed a simple and environment-friendly catalytic process for the oxidation of thiols under mild alkali free conditions. A significant practical advantage of the process is the use of inexpensive cobalt-containing materials derived from the iron-rich soil as heterogeneous catalysts, high-boiling solvents, and molecular oxygen from air as a final oxidant. The choice of a suitable solvent is critically important for the efficiency of the reaction. Weakly basic solvents seem to participate in the activation of the substrate eliminating the need for alkaline co-catalysts, which are corrosive and waste generating. The catalysts provide high product yields at very low loadings and undergo no metal leaching. After the reaction, the catalyst can be easily recovered by the application of an external permanent magnet and re-used several times without any special treatment. We believe that our work contributes to opening the perspectives for the use of abundant natural iron oxides as precursor materials to produce magnetic catalysts. Further studies are targeted towards the applications of the developed materials as catalysts for the aerobic oxidation of other substrates, such as biomass-based olefins.

## Acknowledgments

Financial support from the CNPq, FAPEMIG, and INCT-Catálise (Brazil) is gratefully acknowledged. The authors wish to thank Dr. Claudio Luis Donnici for kind donation of thiols.

## References

[1] B. Basu, S. Satapathy, A.K. Bhatnagar, Catal. Rev. 35 (1993) 571–609.
[2] F. Shirini, M.A. Zolfigol, M. Khaleghi, Mendeleev Commun. 14 (2004) 34–35.
[3] C. Lopes, A. Conzales, F.P. Cossio, C. Palomo, Synth. Commun. 15 (1985) 1197–1211.
[4] A. Shaabani, D.J. Lee, Tetrahedron Lett. 42 (2001) 5833–5836.
[5] K. Nakagawa, S. Shiba, M. Horikawa, K. Sato, H. Nakamura, N. Harada, F. Harada, Synth. Commun. 10 (1980) 305–309.
[6] H. Firouzabadi, N. Iranpoor, F. Kiaeezadeh, J. Toofan, Tetrahedron 42 (1986) 719–725.
[7] M.M. Hashemi, Z. Karimi-Jaberi, Monatsh. Chem. 135 (2004) 41–43.
[8] H. Golchoubian, F. Hosseinpoor, Catal. Commun. 8 (2007) 697–700.
[9] M.M. Hashemi, Z. Karimi-Jaberi, D. Ghazanfari, J. Chem. Res. (2004) 364–365.
[10] M. Kirihara, K. Okubo, T. Uchiyama, Y. Kata, Y. Ochiai, S. Matsushita, A. Hatano, K. Kanamori, Chem. Pharm. Bull. 52 (2004) 625–627.
[11] C.C. Silveira, S.R. Mendes, Tetrahedron Lett. 48 (2007) 7469–7471.
[12] A. Saxena, A. Kumar, S. Mozumdar, J. Mol. Catal. A 269 (2007) 35–40.
[13] V.N. Nemykin, A.E. Polshyna, S.A. Borisenkova, V.V. Strelko, J. Mol. Catal. A 264 (2007) 103–109.
[14] T.V. Rao, K.N. Rao, S.L. Jain, B. Sain, Synth. Commun. 32 (2002) 1151–1157.
[15] S.M.S. Chauhan, A. Kumar, K.A. Srinivas, Chem. Commun. (2003) 2348–2349.
[16] G. Das, B. Sain, S. Kumar, M.O. Garg, G. Murali Dhar, Catal. Today 141 (2009) 152–156.
[17] J.J. Alcaraz, B.J. Arena, R.D. Gillespie, J.S. Holmgren, Catal. Today 43 (1998) 89–99.
[18] D.-e. Jiang, G. Pan, B. Zhao, G. Ran, Y. Xie, E. Min, Appl. Catal. A 201 (2000) 169–176.
[19] H. Liu, E. Min, Green Chem. 8 (2006) 657–662.
[20] H. Mei, M. Hu, H. Ma, H. Yao, J. Shen, Fuel Process. Technol. 88 (2007) 343–348.
[21] A. Shaabani, N. Safari, S. Shoghpour, A.H. Rezayan, Monatsh. Chem. 139 (2008) 613–615.
[22] I.W.C.E. Arends, R.A. Sheldon, Appl. Catal. A 212 (2001) 175–187.
[23] L. Menini, M.J. da Silva, M.F.F. Lelis, J.D. Fabris, R.M. Lago, E.V. Gusevskaya, Appl. Catal. A 269 (2004) 117–121.
[24] M.J. Jacinto, P.K. Kiyohara, S.H. Masunaga, R.F. Jardim, L.M. Rossi, Appl. Catal. A 338 (2008) 52–57.
[25] L. Menini, M.C. Pereira, L.A. Parreira, J.D. Fabris, E.V. Gusevskaya, J. Catal. 254 (2008) 355–364.
[26] M.J. Jacinto, O.H.C.F. Santos, R.F. Jardim, R. Landers, L.M. Rossi, Appl. Catal. A 360 (2009) 177–182.
[27] J.W. Stucki, Soil Sci. Soc. Am. J. 45 (1981) 638–641.
[28] G.A. Sawatzky, F. van der Woude, A.H. Morrish, Phys. Rev. 183 (1969) 383–386.
[29] P.M. Valov, Y.V. Vasilev, G.V. Veriovkin, D.F. Kaplin, J. Solid State Chem. 1 (1970) 215–217.
[30] L.S. Darken, R.W. Gurry, J. Am. Chem. Soc. 67 (1945) 1398–1412.
[31] L.S. Darken, R.W. Gurry, J. Am. Chem. Soc. 68 (1946) 798–816.
[32] X. Li, Y. Cen, H. Liu, Y. Xu, G. Lv, React. Kinet. Catal. Lett. 81 (2004) 313–320.
[33] J. March, Advanced Organic Chemistry: Reactions, Mechanisms, and Structures, forth ed., Wiley, New York, 1992, pp. 250–252.